J Intell Robot Syst (2016) 82:455–466
DOI 10.1007/s10846-015-0268-1

Vibration Based Under-Actuated Bounding Mechanism

Murat Reis

Received: 3 September 2014 / Accepted: 24 August 2015 / Published online: 30 September 2015

Abstract Today's robots are able to perform very limited locomotion tasks by consuming high energy although animals are able to carry out very complicated but stable locomotion tasks using less control inputs and energy. Therefore, it is important to understand the principles of animal locomotion in order to develop efficient legged robots. This paper presents a U-shape visco-elastic beam mechanism that is able to run like a bounding animal when it is actuated by a simple pendulum at the torsional resonance frequency of the elastic body. A simple physical model has been developed to investigate the dynamics of the mechanism and the natural body dynamics of quadrupeds. In the mechanism, a small rotating mass was attached to a DC motor which was mounted on the center of the spine. When this motor is actuated at around the torsional resonance frequency of the elastic body, the robot starts to move and it exhibits a self-organized locomotion behavior. The self-organized locomotion process of the robot does not require any central authority, sensory feedback or external element imposing a planned motion. Comparing the bounding locomotion of the beam mechanism with those of well-known quadrupeds such as a horse, greyhound and cheetah, it can be concluded that the pendulum-driven U-shaped visco-elastic beam displays kinematic behavior similar to a horse, in terms of both experimental and simulation results. Interestingly, this bounding locomotion occurs only if the shape ratio and the actuation frequencies of the beam are close to those of the fastest quadrupeds.

Keywords Vibration · Under-Actuated · Legged locomotion · Quadruped · Elastic · Beam

M. Reis (✉)
Mechanical Engineering Department, Uludag University, Bursa, Turkey
e-mail: reis@uludag.edu.tr

M. Reis
Bio-Inspired Robotics Lab, Institute of Robotics and Intelligent Systems, Swiss Federal Institute of Technology Zurich, Leo D, Leonhardstrasse 27, 8092, Zurich, Switzerland

1 Introduction

In recent years, developing animal-like legged robots has emerged as a new trend in robotics research. Researchers have focused much attention on how to obtain fast and energy efficient locomotion in the basic gaits of bipedal robots, including walking, running and hopping. For example, human-like bipedal walking [1–3], energy-efficient spring mass running [4, 5] and hopping locomotion [6–8] models have been explored by researchers. These studies are helpful to understand the fundamental principles of animal locomotion to a certain extent, and provide several methodologies for improving robot locomotion. Furthermore, biologists have discovered a great deal of information about the gait

patterns of humans and several animals [9–12] suggesting connections between biology and the robotics field. Researchers have also shown a great interest in biologically-inspired fully-actuated smart legged robots due to their maneuverability [13, 14]. Additionally, vibration-based energy-efficient locomotion mechanisms [7, 15] and inertially-actuated gait mechanisms [16, 17] have also been developed in recent years.

One of the design principles to understand adaptability and locomotion behavior is morphological computation [18–20]. This principle states that when a system exploits morphological properties (e.g. shape, stiffness, friction, weight distribution), it is possible to simplify the control architecture and to achieve energy-efficient behavior. Therefore, morphological computation states that incorporating natural body dynamics into robot designs significantly reduces computational efforts. This principle was nicely illustrated by Passive Dynamic Walkers, which could walk down a slope without any actuators [1]. This concept was further extended to passive dynamic running mechanisms, which exhibited running locomotion on a slope in an energy efficient manner similar to human running [21]. However, a common characteristic of these robots is their strong dependence on the environment and lack of behavioral diversity. The stability of the gait patterns against disturbances and the self-organization of the legged locomotion have also been investigated [22–24]. The self-organized locomotion has been obtained by using the natural body dynamics of rigid [1] and elastic elements [25].

Reis and Iida have previously demonstrated that using the natural body dynamics of elastic bodies decreased the impact and damping losses during the hopping locomotion, and they investigated appropriate shapes for the elastic body to obtain different gait patterns [7]. The vibration of the elastic body can be induced by substantially less power when operating at a resonance frequency. It is self-organizing and shows stable movement in four different gait patterns having four, three, two or one phases by using a small periodic actuation with no sensory feedback. The stable gait patterns are based on the intrinsic stability of coupled mechanical dynamics [26].

From this perspective, the main goal of this paper is to investigate the similarity between quadruped animals and the vibration-based visco-elastic beam mechanism. We constructed different shaped and scaled curved beams to understand the effects of the design parameters. We then introduced a simple discrete physical model to simulate the dynamic behavior of the elastic body in Simulink. In this paper, we present simulation and experimental analyses, comparing the results with some of the fastest quadrupeds such as cheetahs, greyhounds and horses.

Section 2 of this paper, introduces the vibration based visco-elastic beam mechanism and the physical model with some assumptions as well as the design variables of the mechanism. Section 3, introduces the simulation and the experimental setup. In Section 4, we compare the experimental results with data collected from video recordings of selected animals. Finally, we discuss the challenges and conclusions of this study in Section 5.

2 Modeling

The bounding mechanism developed for this study consists of a U-shaped visco-elastic beam that is driven by a pendulum (Fig. 1a and b). The dynamics of a visco-elastic beam can be analyzed using discrete elements that are connected to each other by spring-damper elements, and the accuracy of the analyses increases with the number of these discrete elements [27]. Here, the idea we tried to actualize is that the visco-elastic beam can be modeled by using only three links, demonstrating the planar quadruped locomotion (Fig. 1c). Simulink simulations and the experimental results of this study show that such a simple model can capture the dynamics of the visco-elastic beam during locomotion.

The following section describes the conceptual models of the mechanical structures and the motor control and defines some basic parameters to characterize the basic locomotion dynamics in this framework. The mechanism presented in this paper consists of a DC motor, two large feet, and a main body made of a single-piece aluminum beam (E=70 GPa) as shown in Fig. 1b. The U-shaped beam constitutes the leg and spine of the robot, and a rotating mass is attached to the motor, which is mounted on the center of the spine. An actuator controls the direction and the magnitude of the angular velocity of the rotating mass. We used two large feet to ensure that the motion

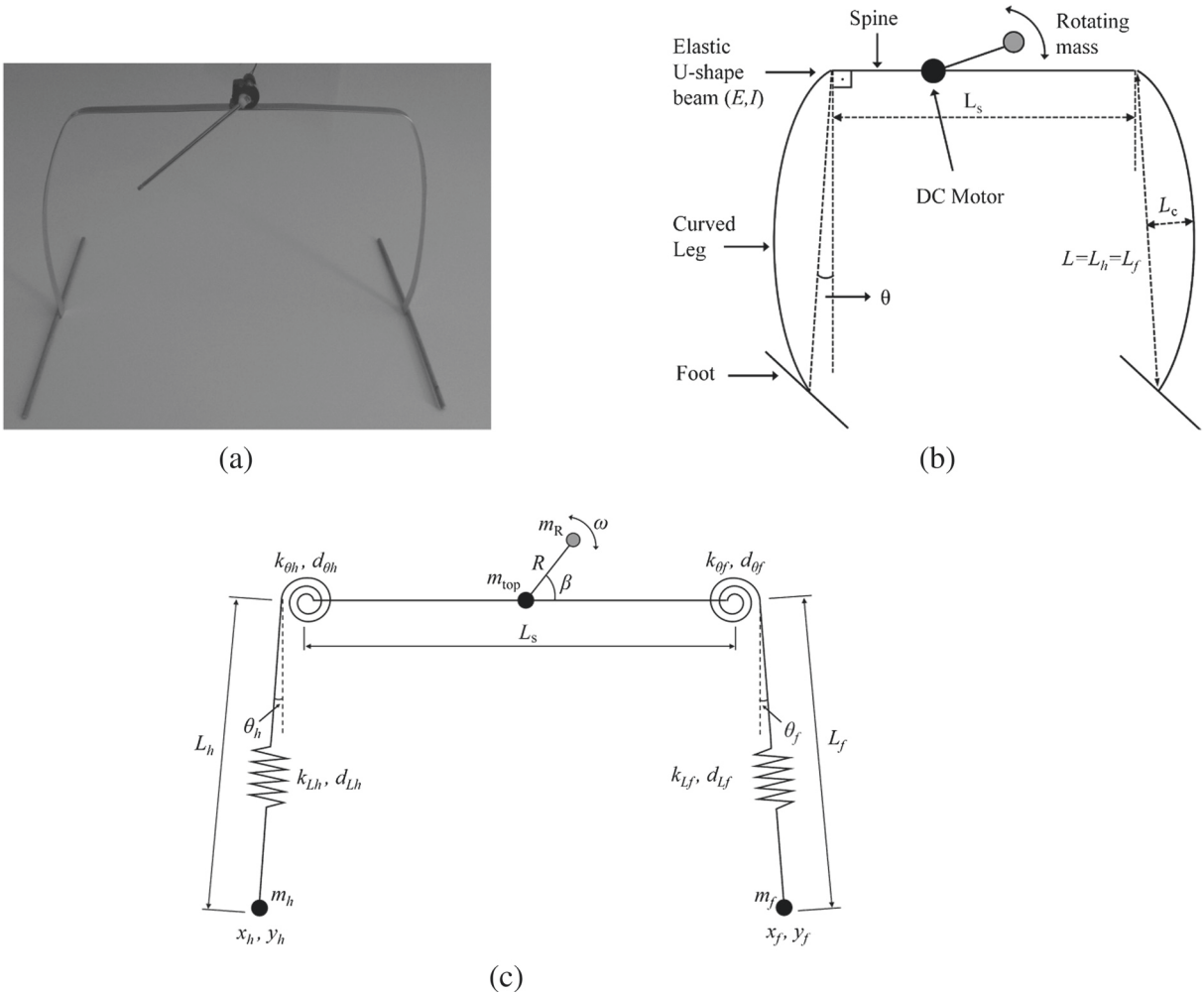

Fig. 1 (**a**) Vibration-based under-actuated bounding mechanism, (**b**) Basic elements of the mechanism, (**c**) A simple physical model for the mechanism

of the robot was in the sagital plane and also incorporated rubber material at the ground contact of the feet in order to gain sufficient ground friction.

2.1 Assumptions and Variables

To construct a conceptual model for these robots in order to perform a systematic simulation analysis, we made the following assumptions: (a) The behavior of this robot can be analyzed in sagittal plane, and the ground contact of each of the feet is a point of contact. (b) The spine of the robot is a rigid beam, and the masses of the spine and the motor can be combined into a point mass at the center of the spine. (c) While the masses of the legs are negligible, each of the feet is a point mass. (d) The rotational behavior between the leg and the spine can be represented by a torsional spring-damper element as shown in the Fig. 1c. (e) The longitudinal deflection of the legs can be represented by a linear spring-damper element. (f) The torsional and longitudinal stiffness above are linear and do not vary with the shape and deflection of the robot body elements.

Based on these assumptions, our model consists of three rigid links connected to each other through torsional and linear spring-damper elements. There are three point masses on these links: first, the masses of the actuator and spine are represented by a point mass m_{top}, which is located at the center of the spine. The other two point masses represent the mass of the front

foot and hind foot which are denoted by m_f and m_h. The shape of the elastic beam can be defined by the natural lengths of the legs (i.e. the leg length when it is unloaded; L_{f0}= L_{h0} = L_0), the curvature of the legs L_c, the spine length L_s and the rest angles between the leg and line perpendicular to the spine (θ_{f0} = θ_{h0} = θ_0). When the elastic beam is without any compression or extension, the natural lengths of the legs and the rest angles of the symmetric robot are defined by L_0 and θ_0. The torsional stiffness and damping of the two joints are represented by k_{θ_f}, k_{θ_h} and d_{θ_f}, d_{θ_h}, respectively. The leg deformation is represented by a linear spring with stiffness k_{Lf}, k_{Lh}, damping d_{Lf}, d_{Lh} and natural length L_0. The rotating mass m_R is connected to the actuator by a bar of length R as shown in Fig. 1c.

In summary, this model consists of 19 mechanical design parameters (i.e. k_{Lf}, k_{Lh}, d_{Lf}, d_{Lh}, k_{θ_f}, k_{θ_h}, d_{θ_f}, d_{θ_h}, θ_{f0}, θ_{h0}, L_{f0}, L_{h0}, L_s, L_c, m_h, m_f, m_{top}, R and m_R), one control parameter (ω), and 18 state variables (i.e. x_f, y_f, x_h, y_h, L_f, L_h, θ_f, θ_h, β, and their velocities) as shown in Fig. 1c and the Appendix.

2.2 Free Vibration Dynamics

The U-shaped beam has two basic vibration modes in planar space as illustrated in Fig. 2. We tried to estimate the resonance frequencies for these two modes both experimentally and analytically. For the experimental estimate, we tested the real-world robots and visually measured resonance frequencies. The analytical solutions were derived based on the formula given below. Here, as the first estimate of resonance frequencies, we assumed no damping in the springs, and the rest angles of both legs were equal to zero ($\theta_0 = 0(rad)$). (see [20]).

One of the simplest analytical solutions of the resonance frequency in the proposed system can be computed when we assume the entire robot to be a bridge-like rigid structure with a pair of upright supporting symmetric legs in parallel (θ_h=θ_f=θ, L_f=L_h=L). In this case, the Lagrangian $\mathcal{L}$ can be derived as:

$$\mathcal{L} = m_{top}gLcos\theta + (1/2)m_{top}(L\dot{\theta})^2 + k_\theta(\theta - \theta_0)^2 + k_L(L - L_0)^2 \quad (1)$$

By differentiating the Lagrangian $\mathcal{L}$ with respect to torsion angle θ, the torsional equation of the motion can be represented by:

$$0 = -m_{top}gLsin\theta + m_{top}L^2\ddot{\theta} + 2k_\theta(\theta - \theta_0) \quad (2)$$

$$\ddot{\theta} + [\frac{2k_\theta\theta - m_{top}gLsin\theta}{m_{top}L^2}] = \frac{2k_\theta\theta_0}{m_{top}L^2} \quad (3)$$

For small angles ($sin\theta \cong \theta$) Eq. 3 can be linearized and torsional resonance frequency ω_θ of the U-shaped elastic beam can be obtained by using the homogeneous part of this differential equation.

$$\ddot{\theta} + \omega_\theta^2\theta = 0 \quad (4)$$

$$\omega_\theta = \sqrt{\frac{2k_\theta - m_{top}gL}{m_{top}L^2}} \quad (5)$$

where k_θ represents the torsional stiffness of the substitute inter-segmental joints between the spine and the legs as shown in Fig. 1c. The expression of k_θ for a cantilever beam is given by EI/L [28]. However, k_θ was determined experimentally in this study, since the elasticity of the aluminum cold-formed beams was not precisely known.

When the Lagrangian $\mathcal{L}$ in Eq. 1 is differentiated with respect to leg length L, we obtain:

$$0 = m_{top}g + m_{top}\ddot{L} + 2k_L(L - L_0) \quad (6)$$

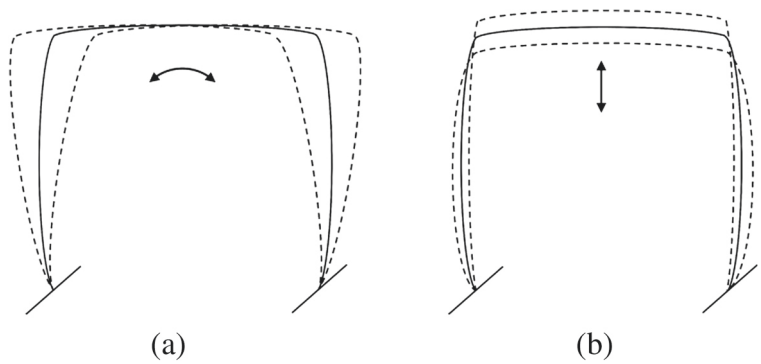

Fig. 2 Exaggerated illustration of the longitudinal and torsional vibrations of the elastic curved beam. (**a**) Torsional vibration trajectories of the curved beam at the stance phase (ω_θ), (**b**) Longitudinal vibration trajectories of the curved beam at the stance phase (ω_L)

$$\ddot{L} + \frac{2k_L}{m_{top}} L = \frac{2k_L L_0 - m_{top} g}{m_{top}} \tag{7}$$

The longitudinal resonance frequency of the elastic beam can be obtained by using the homogeneous part of this equation.

$$\ddot{L} + \omega_L^2 L = 0 \tag{8}$$

$$\omega_L = \sqrt{\frac{2k_L}{m_{top}}} \tag{9}$$

where k_L represents the longitudinal stiffness of the legs as shown in Fig. 1c. Here k_L is the function of the elasticity E, inertia of the cross section of the beam I, length of the robot legs L_0, length of the spine L_s and the curvature of the leg L_c. The effect of the curvature on the stiffness was investigated in earlier versions of this study [7, 20]. The expression for the longitudinal spring forces of the legs was obtained experimentally in various curvature ratios [7].

In order to understand the intrinsic body dynamics derived from the morphological properties, we applied a minimalistic control strategy. We did not use any sensory feedback nor adapt our control scheme based on different phases of locomotion. We used only one actuator in this robot to achieve torsional and longitudinal vibration. The actuator used was a DC motor with a high gear reduction (420 RPM, 0.09 Nm, 50:1 micro MP), which ensured that the angular velocity of the rotating mass was not affected by the robot dynamics. The centripetal force induced by the rotating mass on the robot structure is shown in Eq. 10.

$$F(t) = m_R \omega^2 R \tag{10}$$

The centripetal force generated by the rotating mass induces torsional or longitudinal vibration in the robot structure depending on the magnitude of the angular velocity, rotating mass (m_R) and radius of rotation (R). If it were possible to solve the coupled equations of the motion of the whole system for three different phases analytically, $F(t)$ would be the forcing term on the equation of the spline linkage. For an analytical investigation in planar space, there must be six coupled equations of motion for the three-link system which is shown in Fig. 1c. Additionally, these equations of motion will change with the phases of locomotion (i.e. stance phase, single foot stance phase and flight phase). In this kind of analytical study, every phase's result will be the initial condition for the next phase. Because of these difficulties in an analytical study, we preferred to use a Simulink model to analyze the system.

3 Simulation and Experimental Setup

In the first set of experiments, we built various elastic beams with various shape ratios r_s. Except for the shape ratio, all the other specifications were identical, as shown in Table 1. We managed to obtain bounding locomotion only in a small range of the shape ratios (0.55 - 1.1), as shown in Figs. 5 and 6. In these set ups all U-shaped visco-elastic beams were made of aluminum with rectangular cross-sections of 2×20 mm. The feet were also made of slender aluminum plates and were bolted to the end of the U-shaped elastic beam. The actuator used for these robots was a DC motor with a large gear reduction (50:1). During the experiments, the motor was powered externally with a constant voltage.

In the second set of experiments, we built three robots of different scales, keeping the shape ratio constant ($r_s = 1.1$) as shown in Table 2. In the miniature scale robot, the U-shaped visco-elastic beam and the

Table 1 Specifications used in the design trials (first set of experiments)

L_0	0.4 (m)	R	0.15 (m)
r_c	0.15	θ_0	0.07 (rad)
m_h	0.12 (kg)	m_f	0.07 (kg)
m_R	0.025 (kg)	m_{top}	0.12 (kg)
k_L	200 (N/m)	d_L	0.01 (Ns/m)
k_θ	4 (Nm/rad)	d_θ	0.01 (Nms/rad)
μ_{stick}	0.6	μ_{slide}	0.5
r_s	0.35, 0.45, 0.55, 0.65, 0.8, 0.9, 1, 1.1, 1.2, 1.3		

Table 2 Dimensions used in the design trials (second set of experiments, $r_s = 1.1$)

L_0	0.018 (m)	0.18 (m)	0.5 (m)
R	0.014 (m)	0.09 (m)	0.10 (m)
r_c	0.005	0.008	0.015
θ_0	0.1 (rad)	0.12 (rad)	0.15 (rad)
m_h	0.5 (gr)	20 (gr)	60 (gr)
m_f	0.5 (gr)	20 (gr)	60 (gr)
m_R	0.6 (gr)	8 (gr)	25 (gr)
m_{top}	0.6 (gr)	40 (gr)	150 (gr)

feet were made of 0.2 mm aluminum sheet. In the medium and large scale robots, the beams were made of 1 × 10mm and 2 × 15mm aluminum, respectively, and the feet were made of wood glued to the end of the U-shaped elastic beam (Fig. 3). In the miniature robot, the size of the actuator (1.5V, 6mm, micro motor) limited the scale. In future studies, it is possible to build smaller mechanisms with developments in micro-motor technology. The micro metal gear-motor (50:1) used in the medium and large scale robots of this study was produced by Pololu Robotics and Electronics.

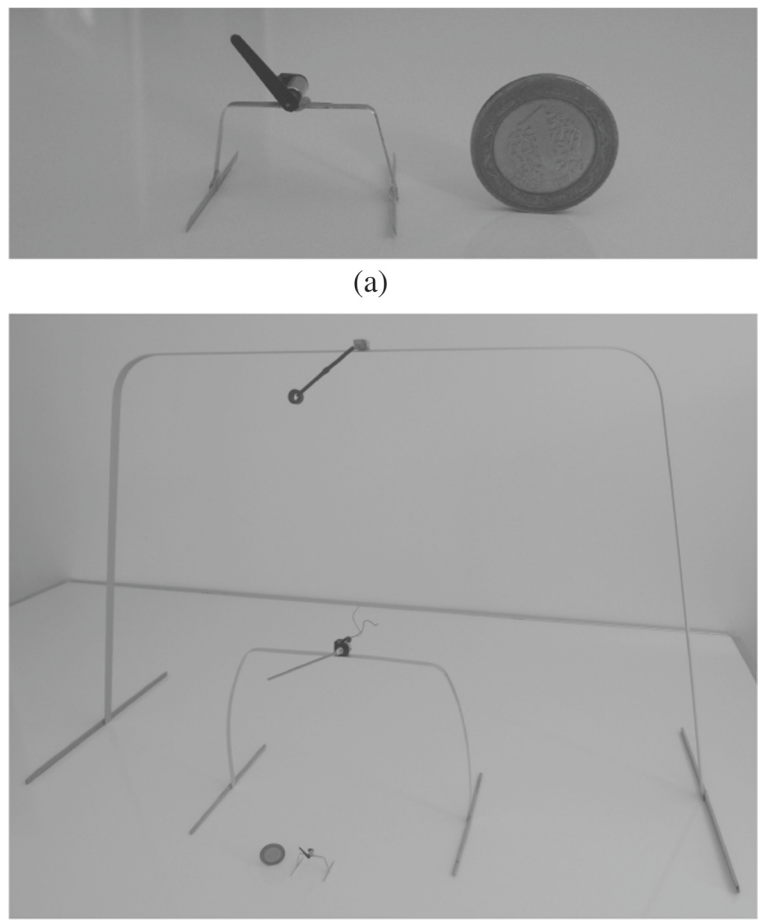

Fig. 3 Photographs of the three scales of robot and coins (All robot beams were made of aluminum beam). (**a**) Miniature robot (Beam cross section=0.2×3mm, robot height=20mm and total weight = 2gr), (**b**) Miniature, medium (Beam cross section=1×10mm, robot height=150mm and total weight = 250gr) and large (Beam cross section=2×15mm, robot height=400mm and total weight = 500gr) scale robots together

In each experiment, we conducted multiple trials with different constant voltages in order to identify the angular velocity of the rotating mass to obtain stable robot locomotion. All of the locomotion experiments shown in this paper were conducted on a 4 m long wooden flat floor. The experimental arena was recorded by a high-speed camera (High Speed Exilim EX-FH20) at 120 frames per second in order to analyze the dynamic motions of the mechanisms.

To understand the dynamics of the U-shaped elastic beam robots, we implemented the physical model of the robot to Matlab (The Mathworks Inc.) containing SimMechanics toolbox. The robot body consisted of a U-shape elastic beam that can be defined as a continuous beam model. A U-shaped elastic beam can also be represented as a series of linear-torsional springs and mass elements. However, we employed a minimalistic model to represent the dynamic behavior of these robots. We used a simple physical model with torsional and linear spring-damper elements for the simulation, as explained in Fig. 1c. For the simulation experiments shown later in this paper, we employed a physically realistic interaction model based on [29].

For each robot, we measured the constant voltage values at which the best locomotion performance could be observed. Because the robots displayed bounding gait patterns, we identified the voltage values that induced the most stable gait patterns.

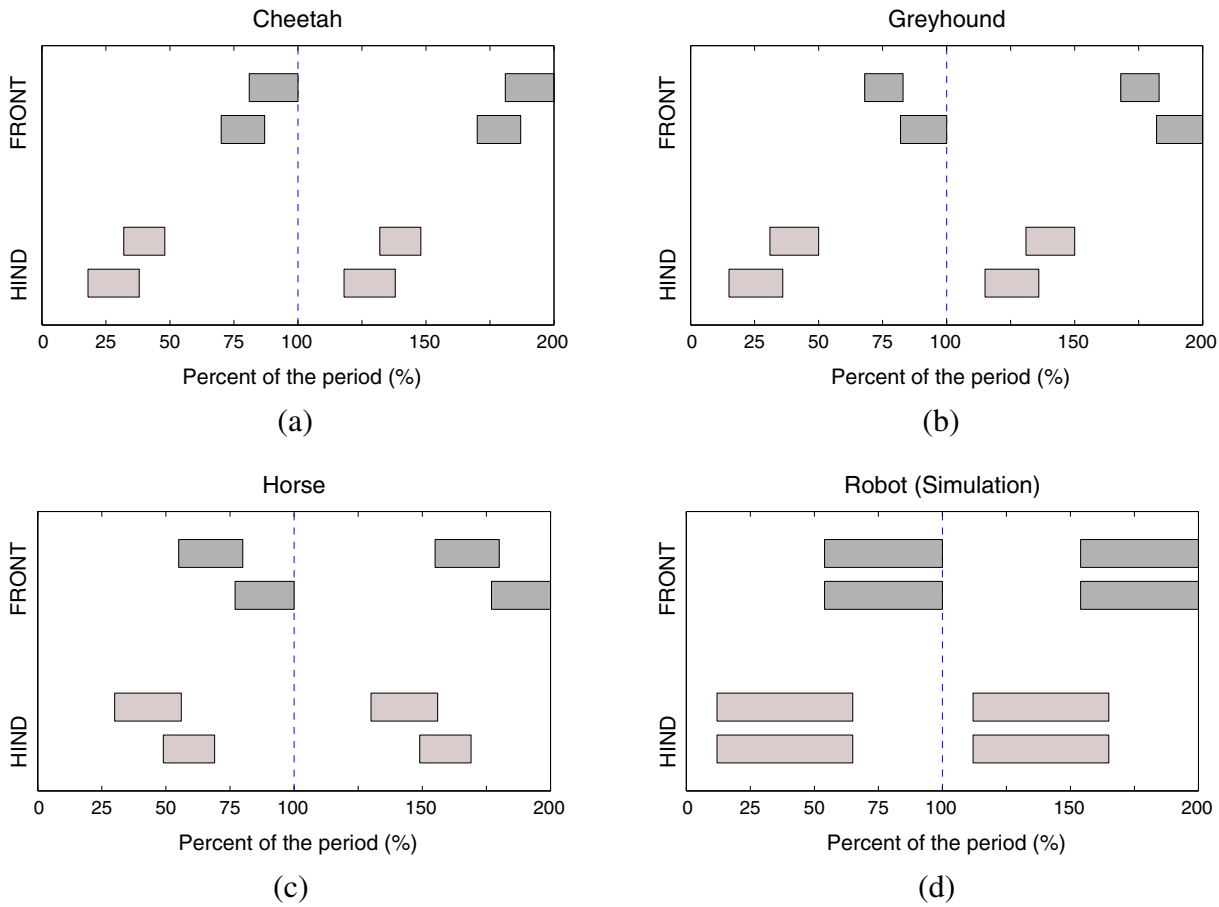

Fig. 4 Gait diagrams (The shaded region indicates that a foot is touching the ground. The data were collected from the high speed camera recordings of the animals). (**a**) Gait diagram of a cheetah bounding. PO: Flight - Hind Stance - Flight - Front Stance, (**b**) Gait diagram of a greyhound bounding. PO: Flight - Hind Stance - Flight - Front Stance, (**c**) Gait diagram of a horse bounding. PO: Flight - Hind Stance - Double Feet Stance - Front Stance, (**d**) Gait diagram of the visco-elastic curved beam bounding, (Simulation results). PO: Flight - Hind Stance - Double Feet Stance - Front Stance

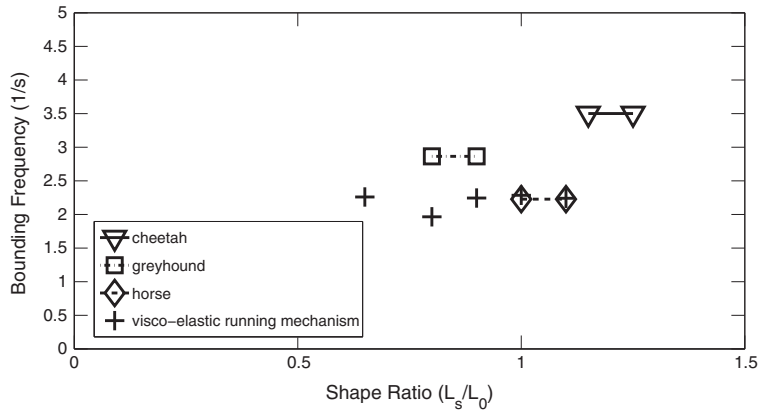

Fig. 5 Bounding frequencies of the quadrupeds and the vibration-based visco-elastic beam mechanisma in various shape ratios which show bounding gait patterns (The mechanism is not able to achieve bounding locomotion when the shape ratio was below 0.65 or above 1.1 in the simulations). (The torsional resonance frequencies of the robot trials were around $\omega_\theta \approx 2.2$ 1/s)

4 Results and Discussion

First, we collected high speed video recordings of cheetahs, greyhounds and horses bounding. Then, we carefully drew the gait diagrams of these animals and measured the locomotion frequencies. The gait diagrams of these three fastest quadrupeds and the visco-elastic beam mechanism are presented together in Fig. 4a,b,c and d. The gait diagrams of these animals and the visco-elastic beam mechanism exhibited four phases in one period.[1] However, the cheetah (Fig. 4a) and the greyhound (Fig. 4b) had two 'flight' phases in one period, while the horse and the vibration-based bounding mechanism had a 'double feet stance' phase unlike the cheetah and the greyhound. There was also an apparent difference between the locomotion frequencies of these two groups (Fig. 5). Here, the cheetah displayed a higher flight phase rate in one period than the horse, and the vibration-based bounding mechanism presented the lowest flight phase rate.

This finding is significant because such a simple under-actuated mechanism showed similar locomotion behavior to that of a horse provided the actuation frequency (torsional free vibration frequency of the mechanism) was around the bounding frequency of the horse.

Although we built various elastic beams with different shape ratios r_s, stable bounding locomotion was achieved in only a small range of shape ratios (0.55 - 1.1) and a small range of frequencies (between 2 − 2.38 1/s) as shown in Figs. 5 and 6. Figure 5 also shows that the actuation frequencies of the robot trials were close to the bounding frequencies of the horse. Furthermore, Fig. 5 also shows that the optimum shape ratios of the visco-elastic beam mechanisms were within the same range as those of these fastest quadrupeds.

4.1 Frequency

Free vibration frequency was used to explore the natural body dynamics of the visco-elastic body of the mechanism. As such, the pendulum was driven at around the torsional resonance frequencies of the robot, which was calculated by using Eq. 5 to make the body move. After conducting up various robot trials, it was found that when the torsional free vibration frequency of the mechanisms was between 2.38 − 3.18 1/s, bounding locomotion was achieved. However, when the torsional resonance frequency of the mechanism was below this range, the robot appeared to be slipping on the ground, and when the torsional resonance frequency of the mechanism was above this range the mechanism displayed chaotic behavior.

It is also seen in Fig. 5 that the bounding frequency of the cheetah (3.5 1/s) is greater than that of the horse (2.38 1/s). This can be explained according to differences in the mass, muscle and claws of these animals. For instance, the cheetah can increase its bounding frequency by using its light body, strong claws and muscles. When we built a visco-elastic beam mechanism with a higher stiffness (in other words, when the torsional resonance frequency was a little higher than 2.38 1/s), the robot's feet began to slip during

[1] See the high speed video record of the bounding locomotion of the visco-elastic beam mechanism at http://www.birl.ethz.ch/Robots/index (Curved Beam Runner).

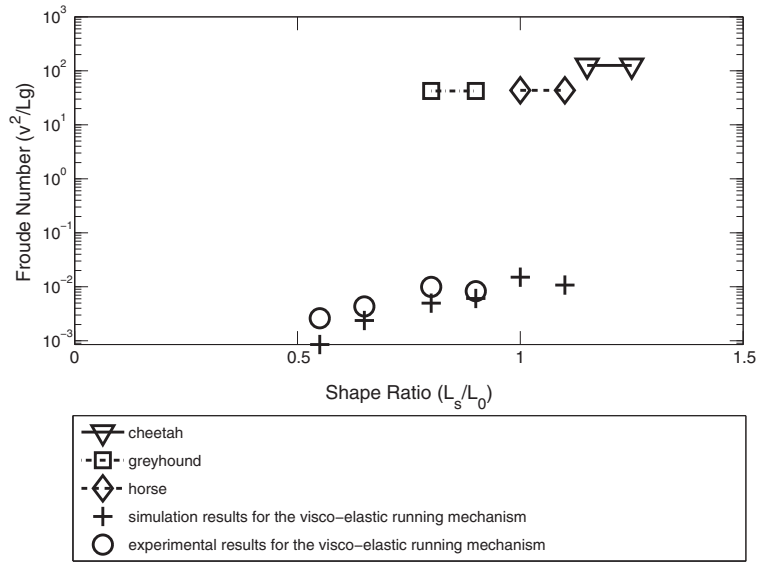

Fig. 6 Froude numbers of the quadrupeds and the vibration-based visco-elastic beam mechanism in various shape ratios which show bounding gait patterns (The mechanism was not able to achieve bounding locomotion when the shape ratio was below 0.55 or above 1.1)

the bounding locomotion, meaning that the locomotion speed and stability decreased. Therefore, it was not possible to achieve stable bounding locomotion when the actuation frequency was significantly different from than those of the quadrupeds in this study, suggesting that. A simple and under-actuated mechanism was able to exhibit dynamic behavior similar to complicated biological organisms.

4.2 Shape

We utilized a dimensionless number called Froude number ($Fr = V^2/gL_0$) to analyze locomotion velocity versus shape ratio r_s [30]. To compare the experimental results, we also conducted the same tests using the simulation model and plotted the results with the data of the three quadrupeds in Fig. 6. As seen in the figure, the Froude number of the biological organisms was higher than those of the robot trials. In this set of experiments, the maximum value of the Froude number of the mechanism was achieved when the shape ratio of the mechanism was close to that of the animals ($r_s = 1$). Consequently, the visco-elastic beam mechanism showed the fastest bounding locomotion performance when the shape ratio was around 1, compared to other shape ratio values.

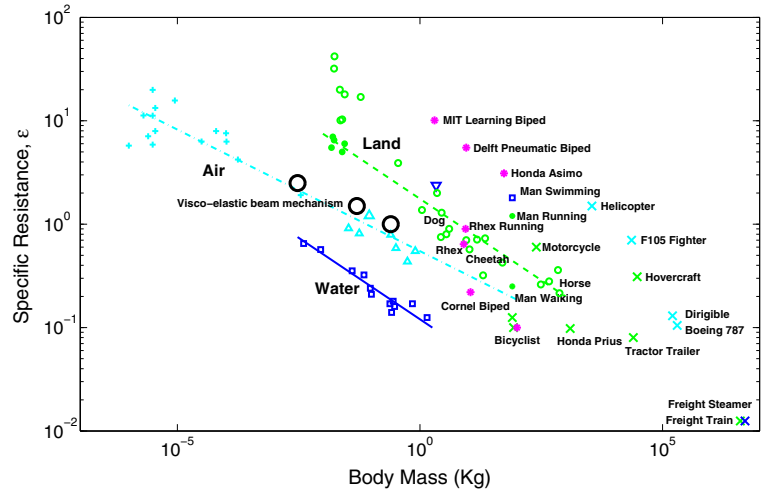

Fig. 7 Specific Resistance (dimensionless cost of transport) versus body mass for various mechanisms and biological organisms (Tucker diagram, [31]). Circles represent visco-elastic beam mechanisms

4.3 Scale

Building a small and energy efficient robot is a challenging task because the smaller the robot is, the lower its energy efficiency becomes. Therefore, the size limitations of a DC motor complicate the question of actuation. As we can see from Fig. [31], the Cost of Transport for small animals is higher than that of big animals. Tucker has explained this issue according to two factors [31]. Small animals, like mice, need more contractions than large animals, like elephants, to cover the same distance. Small animals are also lighter than big animals and reach lower speeds resulting in a higher Cost of Transport.

The energy performance of the under-actuated visco-elastic bounding mechanism is shown using Tucker's diagram [31]. Tucker presented the cost of transport of animals and machines together versus the total body mass of these living and non-living organisms. We took the same diagram but inserted also the results of our three scaled robots. We calculated the power usage of the DC motor on the mechanisms by measuring the voltage and the current during the bounding locomotion. Then we divided the power by the locomotion speed, the mass and the gravity to obtain the dimensionless Cost of Transport. Figure 7 shows that the energy efficiency of the visco-elastic beam mechanism, which in miniature scale was as efficient as flying animals.

5 Conclusion

This paper presents a vibration-based visco-elastic bounding mechanism and investigates the similarity between biologically organisms and the mechanism developed by the researchers. In the analysis, we modeled the continuum body of the robot through a combination of simple linear and rotational spring and damper elements. Even in the simplified model, the simulation and the experimental results of overall behaviors matched reasonably well. The analysis method introduced in this paper can be effectively utilized in complex dynamic robot locomotion because it implies that the overall dynamics of complex body structures can be potentially reduced to simplified models for the ease of analysis and control.

As we point out in this paper, it is possible to scale down the mechanism to miniature form. Through this approach, it is possible to build bounding robots with light bodies or long legs that, are able to move as efficiently as animals. The limiting factors are the motor and the material of the beam. If it is possible to find a smaller DC motor, another way of actuating, or an alternative material for the beams, a total weight of 1 gr or less could be obtained. However, it must be considered that decreasing the weight automatically raises the Cost of Transport.

The self-organized locomotion process of the vibration-based visco-elastic beam mechanism does not require any central authority, sensory feedback or external element imposing planned motion. When comparing the bounding locomotion of the beam mechanism to that of a horse, greyhound and cheetah, it was found that the mechanism displayed similar dynamic behavior, especially with the horse, in terms of both the experimental and the simulation results. This finding is significant because the bounding locomotion occurs only if the shape ratio and the actuation frequencies of the beam are close to those of the fastest quadrupeds, suggesting that animal shape and frequency play major roles in locomotion performance.

Conflict of interests None of the authors has any conflict of interest to report.

Acknowledgments The author would like to thank the Scientific and Technological Research Council of Turkey, TUBITAK and Swiss National Science Foundation. Grateful thanks also go to Mr. Xiaoxiang Yu for assistance on the experimental setup.

Appendix

t Time (s)
x_f, x_h Horizontal positions of the feet (m)
y_f, y_h Vertical positions of the feet (m)
m_{top} Mass of the motor and spine (kg)
m_f, m_h Masses of the front and the hind feet (kg)
m_R Rotating mass (kg)
M Total mass of the robot (kg)
L_f, L_h Length of the front and hind legs (m)
L_s Length of the spine (m)
L_c Horizontal length of the curvature of the legs (m)
L_0 Length of the legs with no load (m)
r_c, r_s Curvature ratio (L_c/L_0) and shaperatio (L_s/L_0)
R Radius of rotation of the rotating mass (m)

θ_f, θ_h Offset angles of the front and hind legs (rad)
θ_0 Offset angle of the legs with no load (rad)
β Angular position of the rotating mass (rad)
k_{Lf}, k_{Lh} Longitudinal stiffness of the curved beam (N/m)
d_{Lf}, d_{Lh} Damping coefficient of the longitudinal stiffness
$k_{\theta f}, k_{\theta h}$ Torsional stiffness of the beam (Nm/rad)
$d_{\theta f}, d_{\theta h}$ Damping coefficient of the torsional stiffness
ω Angular velocity of the rotating mass (rad/s)
ω_L Longitudinal resonance frequency of the U-shape beam (1/s)
ω_θ Torsional resonance frequency of the U-shape beam (1/s)
F Centripetal force of the rotating mass (N)
V Gait speed of the robot (m/s)
E Modulus of Elasticity (N/m^2)
I Moment of inertia (m^4)
g Acceleration of gravity (m/s^2)
μ_{slide} Sliding friction coefficient
μ_{stick} Stiction friction coefficient
$\mathcal{L}$ Lagrangian (Joule)
Fr Froude number
PO Phase order

References

1. McGeer, T.: Passive dynamic walking. Int. J. Robot. Res. **9**(2), 62–82 (1990)
2. Collins, S., Ruina, A., Tedrake, R., Wisse, M.: Efficient bipedal robots based on passive dynamic walkers. Science **307**, 1082–1085 (2005)
3. Blickhan, R., Seyfarth, A., Geyer, H., Grimmer, S., Wagner, H., Gunther, M.: Intelligence by mechanics. Phil. Trans. R. Soc. A **365**, 199–220 (2007)
4. Geyer, H., Seyfarth, A., Blickhan, R.: Spring-mass running: Simple approximate solution and application to gait stability. J. Theor. Biol. **232-3**, 315–328 (2005)
5. Rummel, F.Iida.J., Seyfarth, A.: Bipedal walking and running with spring-like biarticular muscles. J. Biomech. **41**, 656–667 (2008)
6. Blickhan, R.: The spring-mass model for running and hopping. J. Biomech. **22**, 1217–1227 (1989)
7. Reis, M., Iida, F.: An Energy Efficient Hopping Robot Based on Free Vibration of a Curved Beam. Transactions on Mechatronics **19-1**, 300–311 (2014)
8. Yu, X., Iida, F.: Minimalistic models of an energy efficient vertical hopping robot. IEEE Trans. Ind. Electron. **61-2**, 1053–1062 (2013)
9. Roberts, T.J., Kram, R., Weyand, P.G., Taylor, C.R.: Energetics of bipedal running: I. metabolic cost of generating force. J. Exp. Biol. **201**, 2745–2751 (1998)
10. Kar, D.C., Kurien, I.K., Jayarajan, K.: Gaits and energetics in terrestrial legged locomotion. Mech. Mach. Theory **38**, 355–366 (2003)
11. Kokkevis, E., Metaxas, D., Badler, N.I.: Autonomous Animation and Control of Four-Legged Animals. In: Proc. Graphics Interface, vol. 10, pp. 10–17 (1995)
12. Hildebrand, M.: Vertebrate locomotion an introduction how does an animal's body move itself along? BioScience **39-39**, 764–765 (1989)
13. Raibert, M.: Legged robots that balance. Cambridge: MIT Press (1986)
14. Coros, S., Karpathy, A., Jones, B., Reveret, L., Panne, M.: Locomotion Skills for Simulated Quadrupeds. ACM Transaction on Graphics **30-4**, 1–59 (2011)
15. Wang, Z.L.: Bristle mechanism study of a shape reconfigurable brush robot. Industrial Robot: An International Journal **30-6**, 543–551 (2003)
16. Zoghzoghy, J., Alshorman, A., Hurmuzlu, Y.: Inertially Actuated Baton Locomotor. In: ASME Dynamic Systems and Control Conference, pp. 88–97 (2013)
17. Tavakoli, A., Hurmuzlu, Y.: Robotic locomotion of three generations of a family tree of dynamical systems. Part II: Impulsive control of gait patterns. Nonlinear Dynamics **73**, 1991–2012 (2013)
18. Pfeifer, R., Bongard, J.C.: How the Body Shapes the Way We Think. MIT Press, Cambridge (2006)
19. Hauser, H., Ijspeert, A.J., Fchslin, R.M., Pfeifer, R., Maass, W.: Towards a theoretical foundation for morphological computation with compliant bodies. Biol. Cybern. **105**, 355–370 (2011)
20. Reis, M., Xiaoxiang, Y., Maheshwari, N., Iida, F.: Morphological Computation of Multi-Gaited Robot Locomotion Based on Free Vibration. Artificial Life **19**, 97–114 (2013)
21. Owaki, D., Koyama, M., Yamaguchi, S., Kubo, S., Ishiguro, A.: A two-dimensional passive dynamic running biped with knees. IEEE International Conference on Robotics and Automation (ICRA), 5237–5242 (2010)
22. Pfeifer, R., Lungarella, M., Iida, F.: Self-organization, embodiment, and biologically inspired robotics. Science **318**, 1088–1093 (2007)
23. Iida, F., Tedrake, R.: Motor control optimization of compliant one-legged locomotion in rough terrain. In: Proceedings of the 2007 IEEE International Conference on Intelligent Robots and Systems, pp. 2230–2235 (2007)
24. Taga, G., Yamaguchi, Y., Shimizu, H.: Self-organized control of bipedal locomotion by neural oscillators in unpredictable environment. Biol. Cybern. **65-3**, 147–159 (1991)
25. Owaki, D., Koyama, M., Yamaguchi, S., Kubo, S., Ishiguro, A.: A 2-D Passive-Dynamic-Running Biped With Elastic Elements. IEEE Trans. Robot. **27-1**, 156–162 (2011)
26. Maheshwari, N., Yu, X., Reis, M., Iida, F.: Exploiting Free Vibration of an Elastic Beam for Stable Running Locomotion. In: IEEE/ASME International Conference on Advanced Intelligent Mechatronics (2012)
27. Nayfeh, A.H., Pai, P.F.: Linear and Nonlinear Structural Mechanics. Wiley Press (2004)
28. Juvinall, R.: Fundamentals of machine component design, Wiley, 126–127 (1983)

29. Gerritsen, K.G.M., van den Bogert, A.J., Nigg, B.M.: Direct dynamics simulation of the impact phase in heel-toe running. J. Biomech. **28-6**, 661–668 (1995)
30. R. McN. Alexander: The Gaits of Bipedal and Quadrupedal Animals. Int. J. Robot. Res. **3-2**, 49–59 (1984)
31. Tucker, V.A.: The Energetic Cost of Moving About: Walking and running are extremely inefficient forms of locomotion. Much greater efficiency is achieved by birds, fish and bicyclists. Am. Sci. **63-4**, 413–419 (1975)

Murat Reis received the Bachelor's, Master's, and Ph.D. degrees in mechanical engineering from Uludag University, Bursa, Turkey, in 2002, 2004, and 2009, respectively. He worked as a Postdoctoral Researcher in the Bio-Inspired Robotics Laboratory, ETH Zurich, Zurich, Switzerland, between 2010 and 2012. He has been an assistant professor in Mechanical Engineering Department, Uludag University, since 2013. His research interests include dynamics, analytical mechanics, vibration of beams, and mechanics of robot locomotion.